J. Electroanal. Chem., 337 (1992) 147–163
Elsevier Sequoia S.A., Lausanne
JEC 02189

Charging of the Pd/^{n}H system: role of the interphase

S. Szpak *, P.A. Mosier-Boss and S.R. Scharber **
Naval Ocean Systems Center, San Diego CA 92152-5000 (USA)

J.J. Smith
Department of Energy, Washington DC 20585 (USA)

(Received 12 November 1991; in revised form 16 March 1992)

ABSTRACT

The dynamics of transport of electrochemically generated deuterium across the electrode/electrolyte interphase was examined by slow scan (10 mV s^{-1}) voltammetry. The investigation covers the potential range –1.2 to +0.4 V measured vs. an Ag/AgCl reference. It was found that a coupled, two-layer model of the interphase describes the observed behavior as a function of scan rate and electrolyte composition. The effect of chemisorbing species, e.g. CN^- ions, as well as reactive species, e.g. $SC(NH_2)^2$, on the transport across the interphase is also discussed. Results are contrasted with those obtained for light water.

1. INTRODUCTION

The interest in the physicochemical properties of the Pd/^{n}H, n = 1,2, system is prompted by the recent reports that nuclear events are induced by electrochemical compression of deuterium within the palladium lattice [1,2]. The magnitude of this compression, or the degree of loading of the palladium lattice with deuterium during electrolysis, is governed by the processes occurring at, and within, the electrode/electrolyte interphase. These processes both determine the structure of the interphase and define the correct boundary conditions for the solution of the diffusion equation governing the transport of ^{n}H interstitials generated during electroreduction of $^{n}H_2O$ [3,4]. The literature on this subject is voluminous [5–9] but, with a few exceptions [5], limited to light hydrogen. Direct transfer of this information to the transport of deuterium is inappropriate, as shown by microscopic examination of the development of electrode surface morphology following prolonged electrolysis of these two systems [10].

*To whom correspondence should be addressed.
**Permanent address: San Diego Mesa College, San Diego, CA 92111, USA.

The purpose of this communication is to examine the properties and behavior of the palladium/electrolyte interphase in the presence of evolving deuterium and/or hydrogen and to accentuate the differences in interaction between these isotopes and the palladium electrode surface. This is of particular interest in determining the conditions for the initiation of the Fleischmann–Pons effect by the co-deposition technique [11]. We selected slow scan cyclic voltammetry as the primary experimental technique. The advantages of this technique have been pointed out by, among others, Capon and Parsons [6] and Chevillot et al. [9].

2. EXPERIMENTAL

A single-compartment, three-electrode cell was employed throughout. The potential scan was controlled by a PAR, model 362, potentiostat. The reference electrode consisted of a fritted chamber in which an Ag/AgCl wire was immersed in saturated KCl solution in $^{n}H_2O$. This arrangement minimizes Cl^- contamination of the electrolyte of interest. The working electrode was electrodeposited palladium on a gold sphere with a surface area of ca. 5×10^{-2} cm^2, from a bath containing 0.05 M $PdCl_2$ (Aldrich) and 0.3 M LiCl (Mallinckrodt) dissolved in $^{n}H_2O$ (Merck), followed by rinsing in the electrolyte of interest. The use of a gold substrate assured the containment of hydrogen or deuterium within the palladium film and made it possible to vary the thickness and morphology of the palladium deposits in a controlled manner. This approach allowed us to discriminate between bulk and surface effects. A coiled platinum wire was placed around the working electrode to provide a uniform current density distribution. All chemicals were of the highest commercially available quality (analytical reagent grade) and used as received, except when adjusting the pH of the electrolyte. For lowering the pH in light water, concentrated ^{1}HCl was used; for heavy water, the deuterated hydrochloric acid was prepared as follows: $^{2}H_2O$ was added to Al_2Cl_6 (Aldrich) and the gaseous ^{2}HCl was bubbled into a vessel containing $^{2}H_2O$. To increase the pH, Li$O^{n}H$ prepared from metallic lithium (Alfa), was used.

3. STRUCTURE AND DYNAMICS OF THE INTERPHASE

Whenever two phases are brought in contact with each other, an interphase region is created. In electrochemical systems, because of the distribution of electrical charges, the behavior of the Pd/^{n}H-interphase under non-equilibrium conditions can only be described by a multilayer model, in which each layer is of uniform composition and infinitesimal thickness [12]. The structure of the electrolyte side of the interphase associated with the hydrogen evolution reaction and the operating driving forces for the Volmer, Heyrovsky—Horiuti and Tafel paths—in the absence of absorption—has been given by van Rysselberghe [3]. Much less information has been assembled for the solid component of the interphase where the high solubility and mobility of the n H interstitials contribute to the complex nature of the Pd/^{n}H interphase.

One specific example of such a non-autonomous interphase has been considered by Bucur and Bota [13]. They postulated a palladium/electrolyte interphase consisting of two sharply defined regions with discontinuous physicochemical properties. In effect, they considered a common adsorption surface in contact with, and affected by, homogeneous solid and liquid phases. The adsorption plane is in contact with the double layer and with a very thin region, the λ layer, where the concentration of hydrogen is much higher than that which is weakly adsorbed, H(a), or present in the bulk palladium H(II). In the present discussion, although we retain the Bucur—Bota model, we emphasize its non-autonomous character. Thus, we define a transfer zone λ^*, eqn. *(1)*,

$$\lambda^* = \lambda_s + \lambda_e \tag{1}$$

where λ_s and λ_e denote those segments (layers) of the solid and electrolyte phase that actively participate in, and/or dominate, the transport of ^{n}H between them, as illustrated in Fig. 1. By splitting the

interphase into several distinct layers, we are able to identify processes that control the transport of ^{n}H during the potential sweep and the effect of electrolyte composition and electrode surface morphology on that transport. To this end, we have investigated the effect of scan rate, pH, weakly adsorbable ions and surface active species.

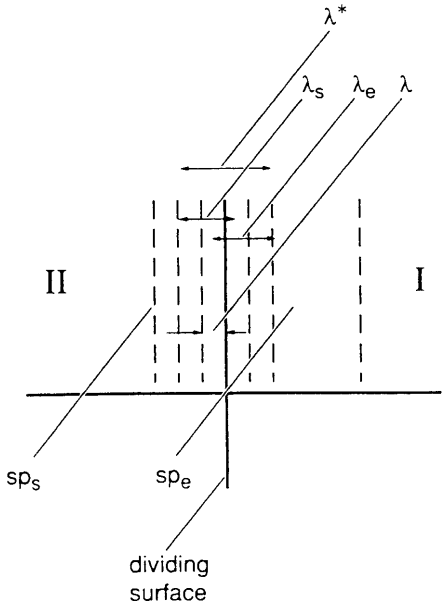

Figure 1. Electrode/electrolyte interphase: λ, Bucur–Bota [13] transfer zone; λ^*, a coupled, two-layer segment of an interphase; λ_s, λ_e, metal and electroylte side of the two-layer segment; sp_s, sp_e, space charge layers.

As required by the non-autonomous character of the interphase, the λ^* layer is an active element of the interphase responding to, and being affected by, the transport across it. For example, the thickness λ^* is affected by charged species, especially those that are strongly adsorbed. It is also affected by the extent of anodic polarization and is attributed to specifically adsorbed negative charges (anions) and oriented $^{n}H_2O$ dipoles within the adsorption layer. The excess negative charges within this layer promotes an accumulation of positive charges (deuterons) held in the transfer layer so that the λ_s layer may extend deeper into the palladium electrode. Also, the anodic current modifies (restructures) the electrode surface by enhancing the transport of ^{n}H which, in our opinion, is an autocatalytic effect.

4. RESULTS AND DISCUSSION

Our experimental results, presented here in the form of voltammograms, were employed to elucidate the behavior of electrochemically generated deuterium on palladium electrodes. The basis for the discussion is the splitting of the interphase into parts reflecting the structure of the metal side, s, and separately, the electrolyte phase, e.

4.1. General Features of the Pd/^{2}H Voltammograms

Typical voltammograms covering the Pd/^{n}H region –1300 to + 400 mV, shown in Fig. 2, are similar to those reported by others [5–9]. Of the two branches, the more revealing and interesting is the anodic branch, because it is here that the characteristic features associated with the ^{n}H transport across the interphase are displayed. An important factor affecting the shape of voltammograms is the electrode surface morphology. On smooth and thin electrodeposits of palladium on gold, peak B is poorly defined compared with peak C. In contrast, both peaks are clearly seen on black palladium

electrodes, i.e. on electrodes prepared at higher current densities. The scanning electron micrograph photograph of the smooth palladium electrode, Fig. 2(a), shows the growth of crystallites on a smooth surface whereas the black palladium surface is porous and consists of an agglomerate of spherical particles of submicrometer size, Fig. 2(b). Therefore, the difference in the shape of voltammograms are due to a surface-to-volume effect of the palladium electrode, a conclusion reached earlier by Chevillot et al. [9]. It was shown that black palladium has an increased number of boundaries where the preferential absorption occurs [10,14], and that hydrogen sorption, I.e. combined adsorption and absorption processes, is much more irreversible in thin films than in bulk palladium [8]. A small cathodic peak, peak D, is observed in the voltammograms on black palladium films but not on smooth palladium. It is unlikely that this peak is due to the reduction of an oxide as the potential scan was terminated prior to oxide formation. Since the black palladium films are thicker and have more surface area as well as more boundaries, peak D is assigned to adsorbed ^{n}H.

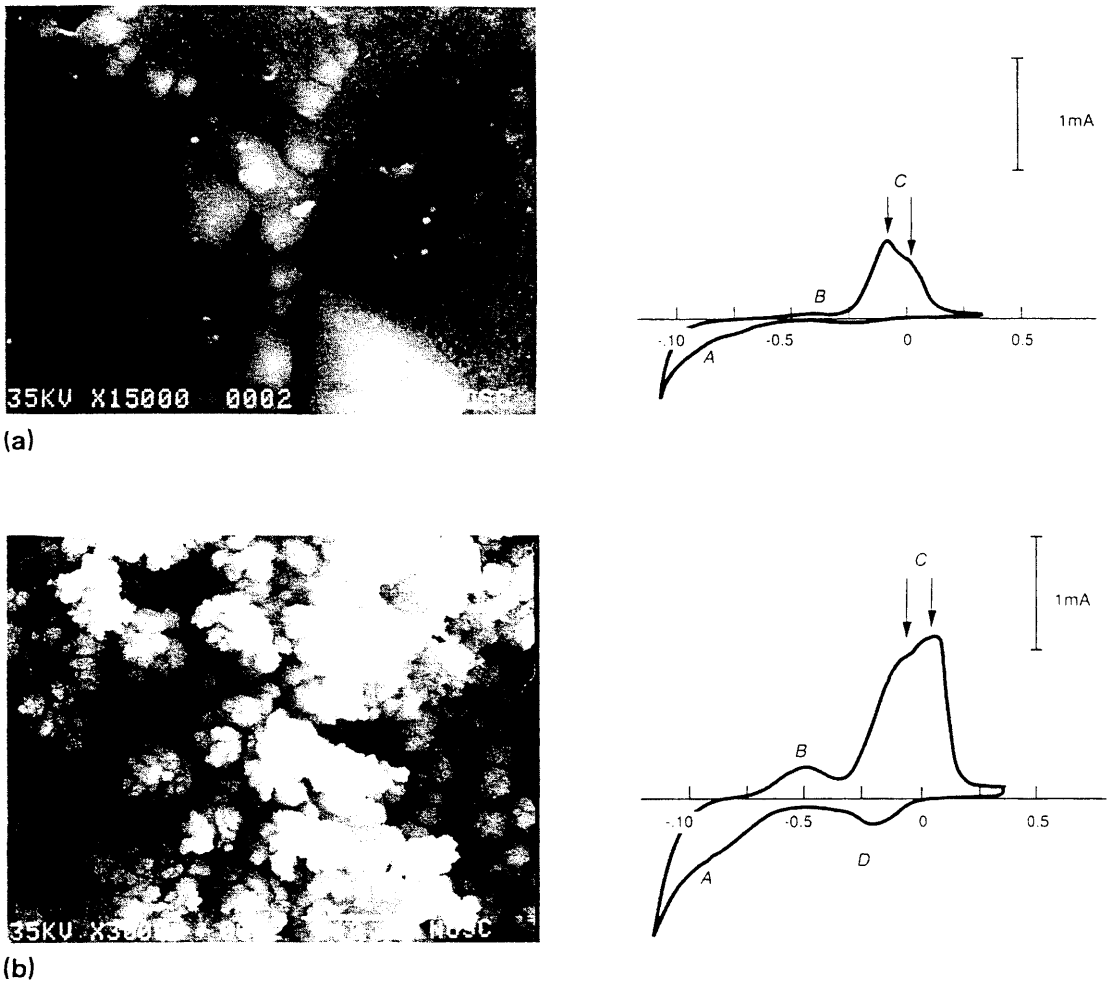

Figure 2. Scanning electron micrographs of palladium electrode surface and corresponding voltammograms, scan rate 10 mVs^{-1}, electrolyte 0.3 M $LiCl/D_2O$: (a) smooth (electrodeposited at 500 μA); (b) black palladium (electrodeposited at 500 μA for 60 min, followed by 50 μA for 3 min).

The positive scan of the voltammograms shows two peaks, labeled B and C, of which peak C is actually composed of two closely spaced peaks, C_1 and C_2. These peaks are generally referred to as "weak" and "strong" adsorption or, more appropriately, to weakly and strongly bound hydrogen. Since peak C occurs at a higher potential and has a higher free energy of adsorption, it is attributed to

strongly bound hydrogen. With regard to Fig. 1, we assign peaks B and C to the reoxidation of ^{n}H in the λ_e and λ_s regions respectively. Since peak C is actually a superposition of two closely spaced peaks, implying that there are two forms of strongly bound ^{n}H, there are at least three forms of hydrogen present in the electrode/electrolyte interphase.

A somewhat better insight into the role of the interphase can be obtained by examining Fig. 3. Figures 3(a) and 3(b) were constructed by varying the potential range scanned. In particular, Fig. 3(a) shows voltammograms that terminate at +400 mV with an increasing span in the negative direction, while Fig. 3(b) illustrates the behavior obtained by anchoring the lower limit at –1200 mV and varying the upper limit. A very small anodic current is observed in the former case, Fig. 3(a), starting the scan at the rest potential, i.e. –118 mV, and terminating at +400 mV. On the return sweep, two peaks appear, at 0.0 mV and at –400 mV, peaks D_1 and D_2. A decrease in the lower limit causes the anodic current to increase and leads to the formation of peaks B, C_1 and C_2; simultaneously, there is a decrease in peaks D_1 and D_2. Different behavior is seen when the upper limit is varied. Termination of the positive scan anywhere within the broad peak B results in a retracing of the anodic segment, see Fig. 3(b). When the scan reversal is initiated at more positive potentials, i.e. outside peak B, a small peak at –150 mV appears which first increases in magnitude and reaches a maximum for scan reversals terminating at the potential of peak C_1. Continuation of scan reversal further into the anodic region, results in a return to a featureless shape of the cathodic segment.

These observations lead to the tentative conclusion that the structure and properties of the λ^* part of the interphase are potential dependent. At potentials less than or equal to +400 mV, the λ_e part of the interphase is electrochemically active (e.g. presence of adsorption sites), provided that no deuterium is present in the λ_s segment. The behavior of the I–η curves, i.e. the appearance of the cathodic peak at –150 mV, shown in Fig. 3(b), suggests the presence within the interphase of charged species containing deuterium, perhaps a $[^{2}H ... {}^{2}H]^{+}$ complex.

Incidentally, there is a degree of similarity between the electrochemical path and that associated with the solid–gas system. In the latter, Auer and Grabke [15] found that three states of the ^{n}H atom exist and play a role in the reaction $H_2 \rightarrow 2H(II)$: first, H(II) residing in the bulk interstices; second, H adsorbed on palladium atoms on the outer surface; third, H(λ^*) adsorbed at the interstices of the inner surface. All these forms are in equilibrium during the adsorption–desorption process. In both electrochemical and solid–gas systems, the dynamic character of the interphase is driven by the energetics associated with the transport of the interstitials.

4.2. Stabilization of Voltammograms

The voltammograms of the Pd/^{n}H region, as in many other complex systems, require several cycles for stabilization. In the present case, as illustrated in Fig. 4, five to ten cycles were usually needed. In general, it was found that the presence of surface active species in the electrolyte reduced significantly the number of cycles needed to stabilize the voltammograms, also shown in Fig. 4. The depth of penetration of diffusing n H interstitials into the palladium electrode is fixed by the stability of the interphase which, in turn, assures stabilization of the voltammograms [16]. This interpretation is in agreement with the concept illustrated in Fig. 1, i.e. when viewing the interphase as composed of two parts, λ_s and λ_e, we conclude that the chemisorbed CN^- ion promotes lesser variation in the concentration of the reactive species with the time dependent overpotential, while the presence of an isopotential point, point P, can be interpreted as the accumulation of ^{n}H within the λ^* layer [17].

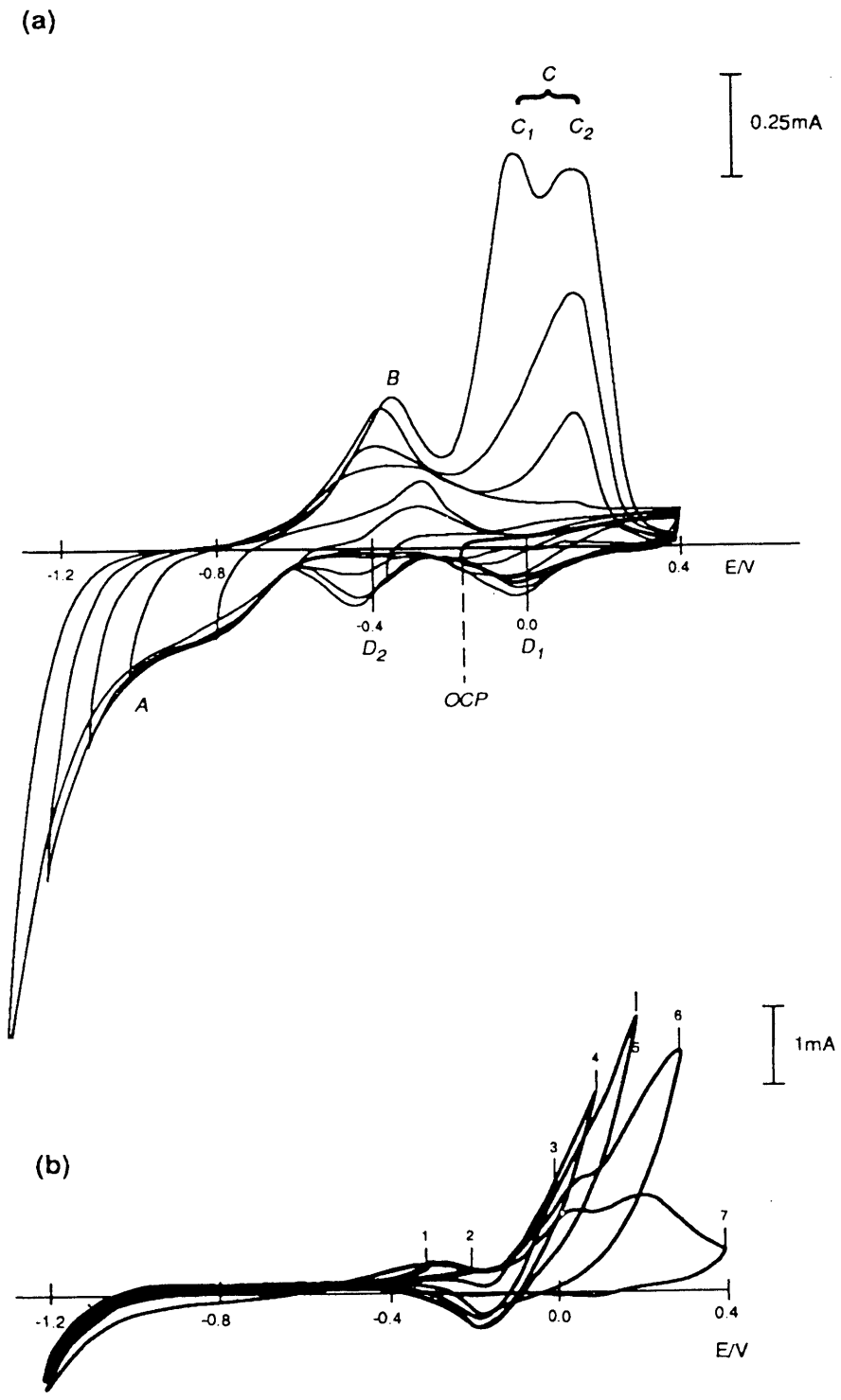

Figure 3. Evolution of voltammograms: (a) as a function of lower scan reversal for a fixed (+400 mV) upper limit potential, reversals at –300, –500, –700, –900, –1000, –1100 and –1200 mV, OCP = –0.118 V vs. Ag/AgCl reference; (b) as a function of upper scan reversal for a fixed (–1200 mV) lower limit potential, reversals at –300 (1), –200 (2), –100 (3), 0.0 (4), +100 (5), +200 (6), and +400 (7) mV.

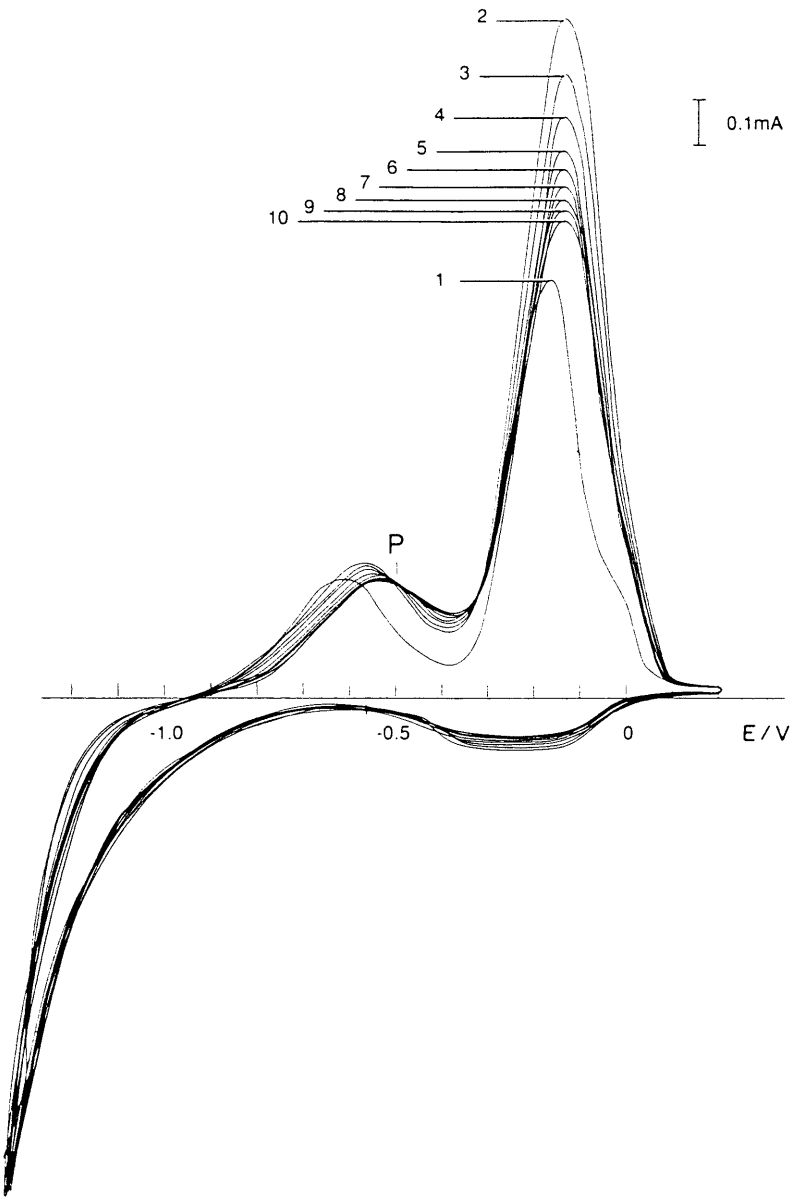

Figure 4. Effect of cycling, electrode surface black palladium, solution 0.3 M^1 Li_2SO_4/D_2O, pH 4, scan rate 10 mVs^{-1}, P isopotential point.

4.3. Effect of Scan Rate

The effect of scan rate is shown in Fig. 5. The major effects of an increase in the scan rate are the disappearance of peak A during the negative scan, an increase in area of peak B, and a shift of peak B to higher potentials during the positive scan. The shift in potential of peak B is limited to a relatively narrow range of scan rates, i.e. to rates greater than 10 but less than 100 mV s^{-1}; the latter scan rate separates the transport phenomena from surface kinetics [13,18]. In contrast, peak C shows relatively little change either in area or position with increasing scan rate. We assume that as interstitial hydrogen, $^{n}H(II)$, leaves the bulk palladium metal and enters the solution phase, it first traverses the λ^* layer (which consists of the first 200–500 Å of the metal [13]) and the adsorption layer. Once in the adsorption layer, the $^{n}H(\lambda_e)$ can either reoxidize or it can enter the space charge layer. In terms of eqn. (1), the effect of scan rate illustrates the influence of the individual parts of the interphase, cf. Fig. 1.

Peak C is due to the reoxidation of strongly bound hydrogen, i.e. hydrogen that resides in the λ_s layer, see Fig. 1. Consequently, if the rate of transport of hydrogen into the λ_s layer is equal to or greater than the rate of the charge transfer, then the concentration of ${}^{m}H(\lambda_s)$ should remain relatively constant. This will result in a peak which shows little or no effect with scan rate, as in the case of peak C. Conversely, peak B is assigned to the reoxidation of weakly bound hydrogen, i.e. hydrogen which resides in the λ_e layer, Fig. 1. If the rate of transport into the λ_e layer is slow relative to the charge transfer, then the opposite effect is expected, i.e. peak B increases in size with increasing scan rate.

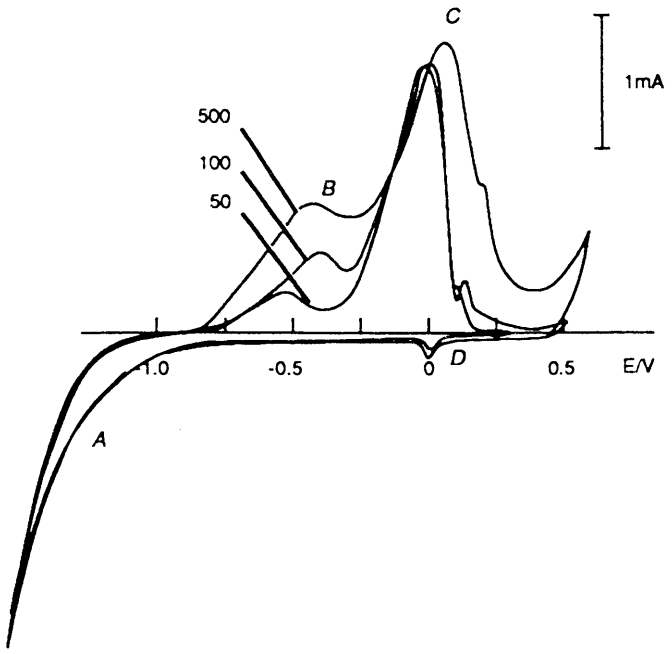

Figure 5. Effect of scan rate, electrode surface black palladium, solution 0.3 M LiCl/D2O, ph 7, scan rates in millivolts per second indicated.

4.4. Voltammograms in Heavy vs. Light Water

One of the conditions believed to prevent the initiation and/or terminate the Fleischmann–Pons effect is the presence of light water in the electrolyte. Its effect on the shape of voltammograms is illustrated in Fig. 6, in particular on the shape and position of peak C. As the concentration of light water is increased, peak C**1** loses its identity (points P_1, P_2, P_3), while peak C_2 increases in peak height and is shifted to higher potential. While there is no change in either the magnitude or position of peak B, peak A becomes an inflection point and a greater number of sweeps are needed for stabilization of the voltammograms as the concentration of light water is increased.

Figure 7(a) shows the effect of adding light water to heavy water during cycling. The results are similar to those described for the mixed ${}^{1}H_2O$–${}^{2}H_2O$ solvents shown in Fig. 6. Finally, the effect of adding heavy water to light water during cycling is shown in Fig. 7(b). It is noted that, as in the previous case, it takes a greater number of sweeps to stabilize the voltammograms shown in Fig. 7. Although more work is needed to establish the effect of mixed solvents on the shape of the voltammograms, nevertheless the present results clearly indicate that exchange of protons and deuterons within the palladium lattice occurs at sufficiently high cathodic overpotentials, (i.e. greater than –1.0 V, the so-called Tafel region).

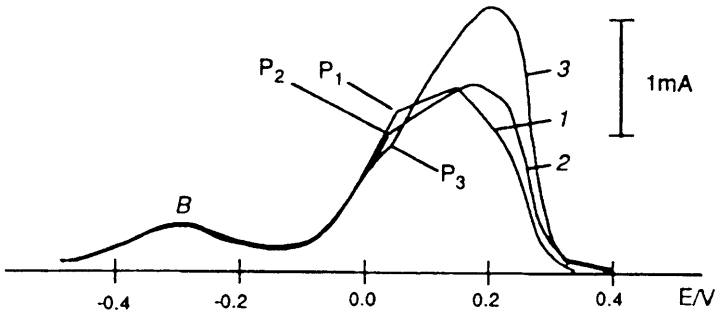

Figure 6. Effect of addition of light water, electrode surface black palladium electrolyte, 0.3 M Li_2SO_4, p^{n}H 12, scan rate 10 mV s^{-1}: curve 1, 10 ml D_2O, 2 ml H_2O; curve 2, 10 ml D_2O, 5 ml H_2O; surve 3, 10 ml D_2O, 10 ml H_2O.

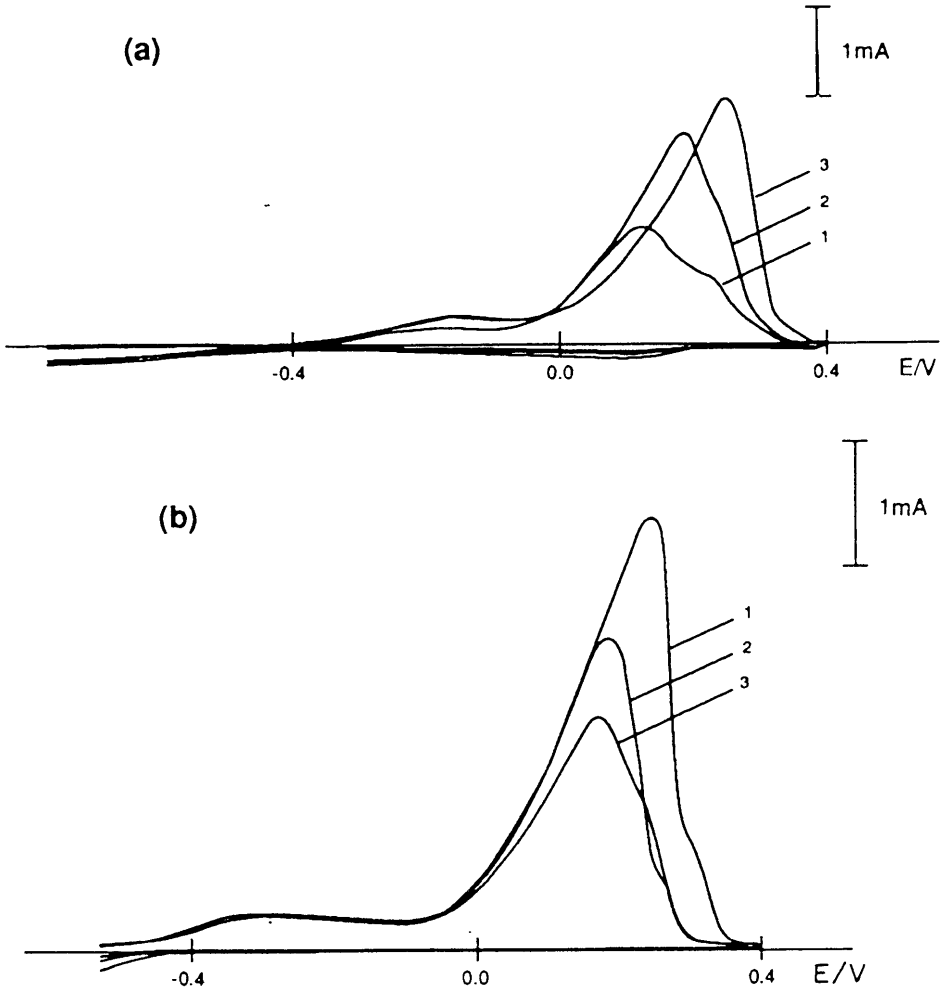

Figure 7. Effect of mixing solvents during cycling. (a) Effect of addition of light water to heavy water: curve 1, 7 ml ^2H_2O; curve 2, add total 3 ml ^1H_2O after the first scan; curve 3, add total 7 ml ^1H_2O, scan taken after cycling for 3h. (b) Effect of addition of heavy water to light water; curve 1, 8 ml ^1H_2O; curve 2, add 8 ml ^2H_2O, scan taken after 1 cycle; curve 3, scan taken after cycling for 45 min. Electrolyte 0.3 M Li_2SO_4, pnH 12, scan rate 10 mV s^{-1}.

4. 5. Effect of pH

Figure 8 illustrates the effect of pH on the voltammograms. In acidic and neutral electrolytes (pH 4 and pH 7) where the charge transfer kinetics are similar, the voltammograms overlap. However, in an alkaline electrolyte (pH 12), where the kinetics are different, there is an enhancement in peak B and a corresponding reduction in peak C with a slight displacement of the latter to a lower potential. The relation between the magnitudes of peaks B and C and their position on the potential scale arises from the interplay between the bulk and surface processes. As a rule, the peaks are better defined in alkaline solutions and the observed effects are greater for electrolytes containing Cl^- ions. In terms of the concept of the λ^* phase, in alkaline solutions containing Cl^- ions, becomes dominant.

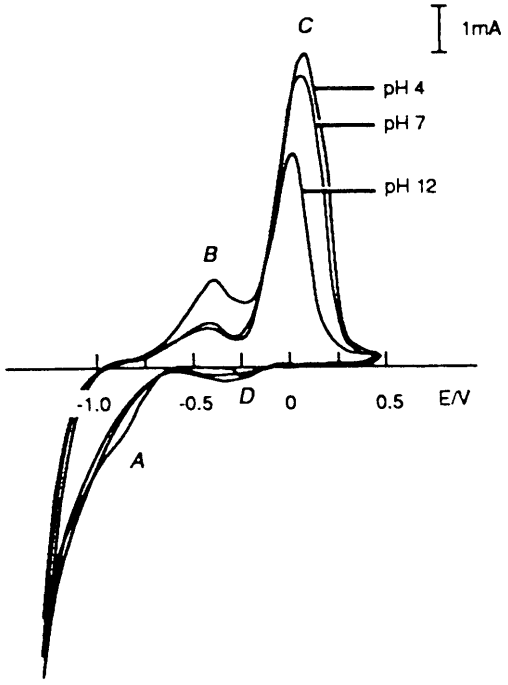

Figure 8. Effect of pH, electrode surface black palladium, solution 0.3 M Li_2SO_4/H_2O, scan rate 10 mV s^{-1}, pH indicated.

4.6. Effect of Weakly Adsorbable Ions

The effect of weakly adsorbed anions on the voltammograms was investigated by changing electrolyte composition but not ionic strength. In particular, Fig. 9(a) illustrates how a change in an anionic species affects the shape of the voltammo- gram. In slightly acidic and neutral electrolytes (at pH 4 or pH 7), no differences between the voltammograms obtained for KCl and K_2SO_4 electrolytes are observed. However, at pH 12 the .presence of Cl^- ions enhances peaks B and D, with the corresponding changes in peak C. The appearance of peak D indicates that not all the ^{n}H atoms are transported into the palladium lattice. Therefore, Cl^- in the presence of O^nH^- inhibits diffusion of ^{n}H into the metal, a conclusion reached earlier by Breiter [19]. The change in peak C indicates that the adsorbed Cl^- ion in alkaline electrolytes competes with O^2H^- ions. According to Bucur and Bota [13] the thickness of their postulated layer is greatly affected by the adsorption properties of the anionic species occurring in solution.

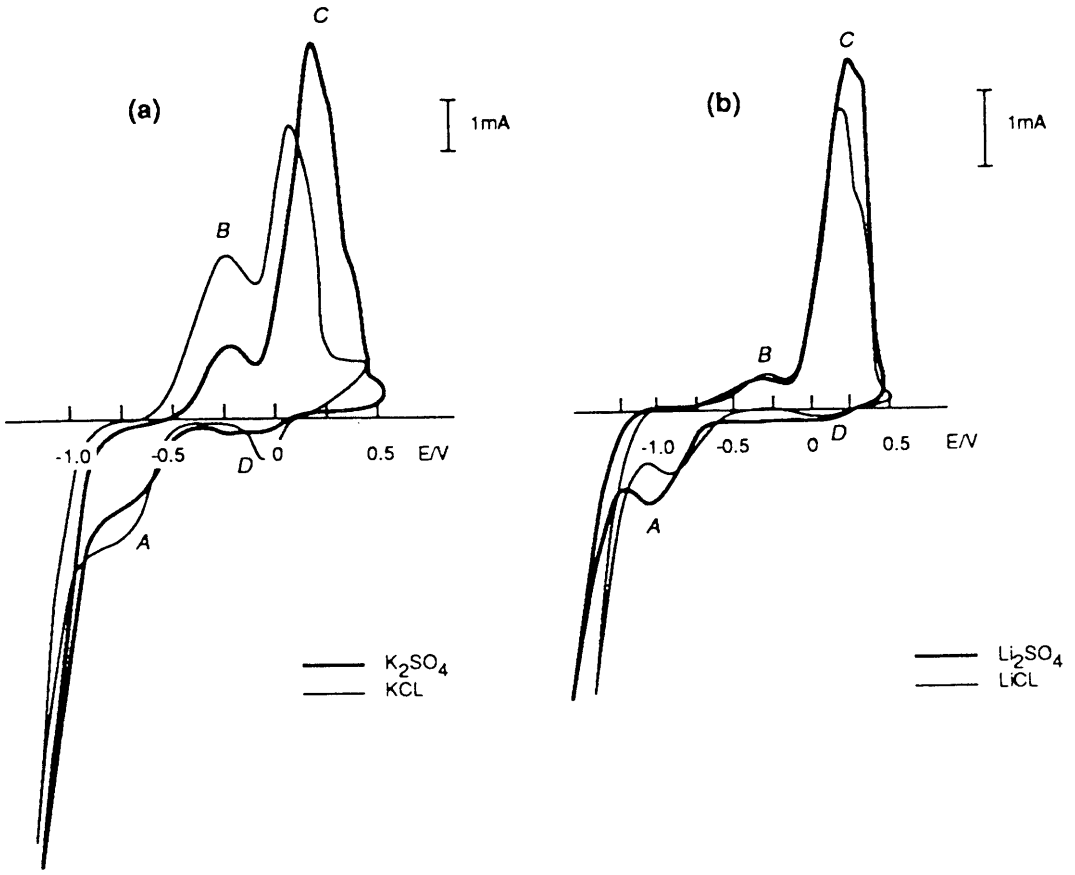

Figure 9. Effect of the supporting electrolyte, scan rate 10 mV s^{-1}, electrode surface black palladium, pH 12, solvent D2O: (a) 0.3 M potassium salts (Cl^-, SO_4^{2-}); (b) 0.3 M lithium salts (as above), SO_4^{2-} thick line, CL^- thin line.

When the K^+ ion is replaced by Li^+, no significant differences are observed in the voltammograms, as shown in Fig. 9(b), regardless of the pH or the counterion. Such behavior is attributed to specific adsorption of the Li^+ ion. The influence of electrolyte composition and pH on peaks B and D is related to the adsorbability of the species present in the electrolyte, a conclusion also reached by McBreen [5].

4.7. Effect of Surface Active Species

Among species strongly adsorbed on the palladium electrode surface are the CN^- ion and thiourea. Figure 10 shows the effect of adding KCN to the electrolyte, i.e. the effect of the CN^- ion lying flat on the palladium surface [20]. Within the potential range examined, the addition of CN^- results in a loss of peaks A, B and D as well as loss of the component of peak C which occurs at a more negative potential . However, with positive scans terminated at higher positive potentials, e.g. at 1.0 V vs. Ag/AgCl reference, shown in Fig. 10, peaks A and D reappear. Evidently, a strongly adsorbed (chemisorbed) species modifies the structure of the electrode/electrolyte interphase in a different manner than less strongly adsorbed species. In particular, the presence of CN^- does not prevent the diffusion of ^2H atoms into the palladium lattice, in agreement with the results obtained by McBreen [5]. It appears, however, that the CN^- ion does inhibit the outgassing of $^2H(\lambda^*)$ out of the λ_s into the λ_e layers. The single anodic peak observed in the voltammogram is attributed to reoxidation of ^2H within the palladium layer in closest contact to the solution phase, i.e. the λ_e layer. Therefore, it would

appear that the two overlapping components of peak C are assigned to reoxidation of $^{2}H(\lambda_e)$ and in the $^{n}H(\lambda_s)$ layers respectively.

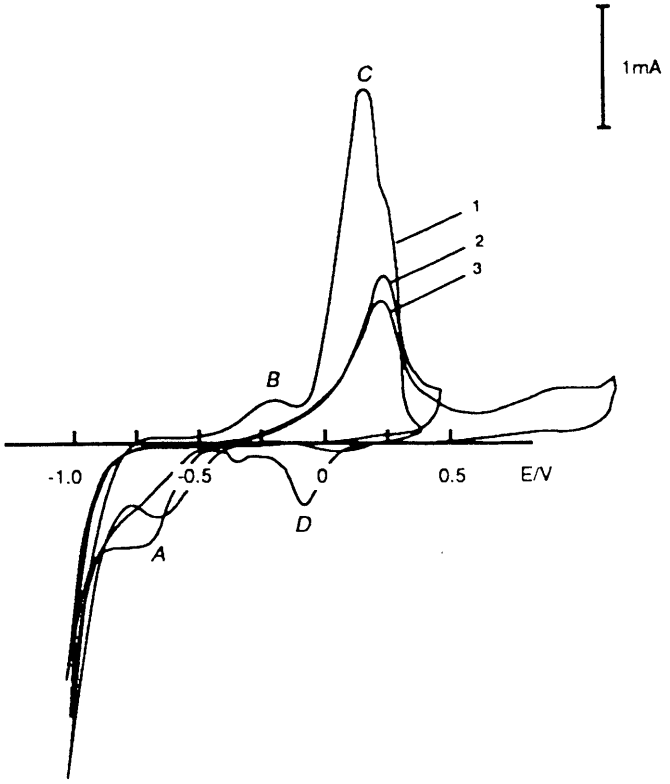

Figure 10. Effect of addition of CN^{-}. Electrode surface black palladium, solution 0.3 M Li_2SO_4/D_2O, pH 12, scan rate 10 mVs^{-1}, final concentration of KCN was 10^{-3} M: curve 1, before addition of KCN; curve 2, after addition of KCN positive scan terminated at +500 mV; curve 3, positive scan terminated at +1000 mV.

The addition of thiourea, ca. 10^{-3} M, to the electrolyte greatly alters the voltammograms, as shown in Fig. 11 where the voltammograms obtained in the absence and presence of $SC(NH_2)_2$ are displayed. With the addition of thiourea, the anodic peak B becomes an inflection occurring at ca. 300 mV more positive and the much broader peak C, also displaced by 300 mV, retains its structure (the two closely spaced peaks). At still higher positive potentials, a new peak is observed. Of note is the dependence of the shape of the negative branch of the voltammograms. When the positive sweep is terminated before substantial oxidation of adsorbed and/or absorbed ^{2}H occurs, the negative sweep retraces the positive sweep. When terminated at the point of inflection, a peak in the negative sweep appears which is shifted more negative by ca. 300 mV with respect to the peak observed in the absence of thiourea. The magnitude of this peak decreases as the terminating potential is more positive, until the terminating potential exceeds 1.2 V, at which point two new peaks appear. These latter two peaks may be due to the reduction of sulfur compounds adsorbed on the surface or may indicate surface restructuring associated with electrode polarization [14].

5. CLOSING REMARKS

The quantitative description of the ^{n}H transport across the interphase requires that both the interphase structural features and the kinetics of the processes, which lead to the formulation of applicable boundary conditions, be specified. Two models have been advanced. In one approach, Bucur and Covaci [18] formulated a set of equations describing the transport of hydrogen from the electrode

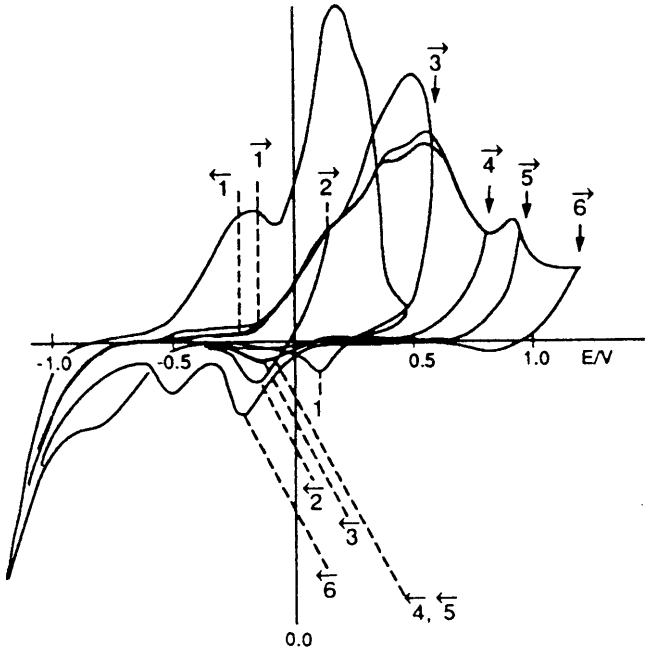

Figure 11. Effect of addition of $CS(NH_2)_2$, electrode surface black palladium, solution 0.3 M Li_2SO_4/D_2O, pH 12, scan rate 10 mV s^{-1}, final concentration of $CS(NH_2)_2$ was 10-3 M.

interior to the charge transfer plane by invoking mass balance equations. A more general discussion of the transport was given recently by Szpak et al. [4] in which they adopted a modified van Ryssel-berghe [3] concept of the interphase region as representing the Pd/^{n}H$_2$O system by including absorp-tion process(es), i.e. the penetration of ^{n}H into the palladium lattice. While discussing the properties of the interphase, it is important to note that the movement of the absorbed interstitial is accompanied by profound local changes arising from lattice expansion, especially at the $\alpha \rightarrow \beta$ transition plane [21].

Qualitatively, during the negative scan, as the concentration of ^{n}H(a) increases with the applied overpotential, so does the amount of ^{n}H(λ^*) which, in turn, diffuses into the bulk metal, ^{n}H(II). Dur-ing the discharge, the elementary processes are reversed in direction while retaining the same mecha-nism within the bulk electrode. On the surface, ^{n}H(λ_e) undergoes oxidation with the distribution of the driving force depending on the reaction path. In particular, at low anodic current densities, an equilibrium H(λ_s) $\rightarrow$ H(λ_e) can be assumed. At higher currents, however, a non-equilibrium situation may develop owing to the slowness of either the transfer step or diffusion through the palladium lat-tice. In such a case, the rate-determining step is identifiable.

General features of the voltammograms pertaining to the Pd/^{n}H$_2$O system, i.e. (i) peaks are observed in the positive direction but rarely in the negative, (ii) a number of scans is required to stabi-lize a voltammogram, and (iii) a coupling between the forms of adsorbed–absorbed ^{n}H exists, indi-cate strong involvement of the interphase. The lack of distinct features during the negative scan sug-gests that the ^{n}H atom, formed upon reduction of ^{n}H$_2$O, is transported across the λ_s layer directly into the palladium lattice. The existence of the inflection point A, Fig. 4, appearing in the course of light water reduction which in heavy water often becomes a well defined peak, Fig. 9(b), we propose is attributed to the difference in the number of reactive sites on the electrode surface arising from the difference in the rate at which the ^{n}H cross the λ_s layer, this rate being faster for light hydrogen. The elimination of this peak upon addition of CN^- ions means that the total number of sites has been

reduced. It should be noted that the shape of peak A is strongly dependent upon the history of the electrode, scan rate, pH and solution composition. This suggests that this peak arises from the restructuring of the λ^* layer occurring at more positive potentials, a conclusion reached earlier by Bucur and Bota [13].

The complex nature of the interaction between the λ_e and λ_s layers is further shown by' the shape of voltammograms obtained in the presence of thiourea. Here, the formation of ··· S bonds 'affects not only the space charge layer in the λ_e but also the λ_s segments of the interphase. In conclusion, we suggest that, in the course of the palladium electrode charging, the interphase is not a passive element but an active participant.

ACKNOWLEDGEMENT

The authors wish to express their gratitude to Drs. D.R. Rolison (NRL) and R.J. Nowak (ONR) for penetrating discussions. Special thanks to Dr. Frank Gordon (NOSC) for his interest, encouragement and support.

REFERENCES

1. M. Fleischmann, S. Pons and M. Hawkins, J. Electroanal. Chem., 261(1989)301.
2. M. Fleischmann, S. Pons, M.W. Anderson, L.J. Li, and M. Hawkins, J. Electroanal. Chem., 287 (1990)293.
3. P. van Rysselberghe, Some Aspects of the Thermodynamic Structure of Electrochemistry, in J.O'M. Bockris (Ed.), Modern Aspects of Electrochemistry, Vol. 4, Plenum, New York, 1966.
4. S. Szpak, C.J. Gabriel, J.J. Smith and R.J. Nowak, J. Electroanal. Chem., 309(1991)273.
5. J. McBreen, J. Electroanal. Chem., 287(1990)279.
6. A. Capon and R. Parsons, J. Electroanal. Chem., 39(1972)275.
7. R.R. Adzic, M.D. Spasojevic and A.R. Despic, J. Electroanal. Chem., 92(1978)31.
8. J. Horkans, J. Electroanal. Chem., 106(1980)245.
9. J.-P. Chevillot, J. Farcy, C. Hinnen and A. Rousseau, J. Electroanal. Chem., 64(1975)39.
10. D.R. Rolison and P.P. Trzaskoma, J. Electroanal. Chem., 287(1990)375.
11 S. Szpak, P.A. Mosier-Boss and J.J. Smith, J. Electroanal. Chem., 302(1991)255.
12 R. Defay, I. Prigogine and A. Bellemans, Surface Tension and Adsorption, Engl. trans., D.H. Everett, Longmans, Green & Co, London, 1966.
13 R.V. Bucur and F. Bota, Electrochim. Acta, 26 (1981)1653; 27(1982) 521; 28 (1983)1373.
14 S. Szpak and P.A. Mosier-Boss, unpublished results, 1990.
15 W. Auer and H.J. Grabke, Ber. Bunsenges., 78(1974)58.
16 H.S. Carslaw and J.C. Jaeger, Conduction of Heat in Solids, Oxford University Press, London, 1948.

17 D.F. Untereker and S. Bruckenstein, Anal. Chem., 44(1972)1009.

18 R.V. Bucur and **I.** Covaci, Anal. Chem., 30(1985)1237.

19 M.W. Breiter, J. Electroanal. Chen1., 90(1978)425.

20 J. Sommers, M.E. Kordesch, Th. Lindner, H. Conrad, A.M. Bradshaw and G.P. Williams, Surf. Sci., 188 (1987) L693.

21 M. V. Stackelberg and P. Ludwig, Z. Naturforsch., 19A (1964)93.